

# FLUX DIFFUSION AND ACCELERATION IN A HIGH-CURRENT MODIFIED BETATRON<sup>†</sup>

JOHN M. GROSSMANN,<sup>‡</sup> WALLACE M. MANHEIMER,

*Plasma Physics Division, Naval Research Laboratory, Wash., D.C. 20375, U.S.A.*

and

JOHN M. FINN

*University of Maryland, College Park, MD 20792, U.S.A.*

*(Received January 30, 1984; in final form May 29, 1984)*

An analytic and numerical scheme is developed to determine self-consistent equilibria in modified betatrons. As the beam undergoes adiabatic changes, its behavior is determined by a series of time-dependent equilibria. At any time, these equilibria are characterized by the number of particles in a drift ( $P_\theta$ ) surface, and the toroidal flux through a  $P_\theta$  surface. In this paper, the evolution of the drift surfaces is followed during beam acceleration and self-flux diffusion, and beam equilibria are found for various levels of flux-diffusion compensation. As the beam accelerates, it reaches a certain energy at which it makes a transition from diamagnetic to paramagnetic poloidal drift. This transition is characterized by a change in topology of the  $P_\theta$  surfaces. Depending on the change in shape at transition, the new  $P_\theta$  surface can either be confined in the liner or run into the liner. Conditions for confined orbits at the transition are given for parameters of the NRL modified-betatron experiment. During flux diffusion, it is found that large adjustments in external fields are necessary to maintain equilibrium. It may be possible to overcome this difficulty by placing a set of external coils at the liner to compensate for the decaying eddy currents. When the distribution of currents in these coils mimic the surface currents exactly, no adjustments in external fields are necessary. However, beam equilibrium is very sensitive to the azimuthal error in this distribution.

## I. INTRODUCTION

The evolution of a high-current electron beam in a modified betatron<sup>1-4</sup> during self flux diffusion and acceleration is described in this paper. An investigation is also made of the effect on beam equilibrium of the presence of a discrete set of coils designed to compensate for flux diffusion. Our results are based on calculations of equilibrium solutions of the cold-fluid equations and their adiabatic evolution, as described in earlier works.<sup>5,6</sup>

In Fig. 1, we show a schematic diagram of the modified betatron together with the experimental parameters we use (unless otherwise specified). The motion of electrons is broken into several time scales: the poloidal ( $r-z$  plane) cyclotron motion in the toroidal ( $B_\theta$ ) field with period of about  $10^{-11}$  sec, the toroidal major rotation in the vertical field of about  $10^{-8}$  sec, the poloidal drift,  $v_p$ , in the  $B_\theta$  field of about  $10^{-7}$  sec, the time scales for flux diffusion on the order of  $10^{-4}$  sec, and finally the time scale for acceleration  $\sim 10^{-3}$  sec. Notice that from about the first microsecond to the first

<sup>†</sup> Work supported by ONR and NRC

<sup>‡</sup> NRC-NRL Associate

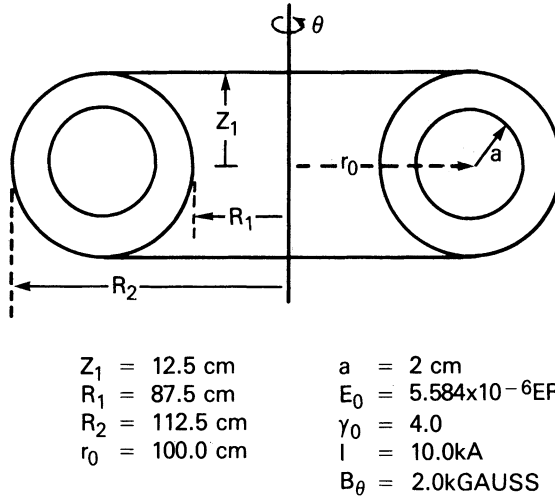


FIGURE 1 Modified betatron schematic with typical parameters.

100 microseconds of the beam's existence, the dominant process is the diffusion of the beam self fields through the liner walls. A crucial issue for the modified betatron then is whether the beam can survive this flux diffusion. If it cannot, external regulating coils are needed and the question becomes: just how accurate must the current in the regulating coils be controlled? This paper will address this issue. In contrast to concurrent studies<sup>7-10</sup> using particle simulations, the very long time scales involved in flux diffusion and acceleration dictate a fluid description that averages out the individual motion of electrons and studies the adiabatic development of the beam on time scales longer than the poloidal drift period.

In our axisymmetric system at steady state, all the forces on the beam are in the poloidal plane.<sup>11</sup> The outward  $\gamma v_\theta^2/r$  centrifugal force and hoop stresses are balanced by the inward  $v_\theta \times B_z$  force and the defocusing effects of the self electric field and image charge are balanced by the focusing forces due to the external index  $\eta$ , the poloidal self magnetic pinch force ( $V_\theta \times B_p$ ) and the  $v_p \times B_\theta$  force. In a high-current betatron, the repulsive electrostatic forces dominate the attractive forces due to external and magnetic pinching (at sufficiently low  $\gamma$ .) Thus, the additional  $v_p \times B_\theta$  is necessary for equilibrium and the resulting electron drift is diamagnetic. The other forces in the poloidal plane, the inertia and centrifugal forces due to poloidal motion, are neglected in our formalism because they are negligible when the toroidal field is sufficiently large and the density and energy sufficiently small.

In Refs. [5] and [6], it is shown that the fluid canonical angular momentum  $P_\theta$  characterizes the equilibria because many important fluid quantities are functions of  $P_\theta$  and because surfaces of constant  $P_\theta$  are drift surfaces of single electrons. It follows that beam equilibria can only exist on those  $P_\theta$  surfaces that are closed within the confining conducting wall.

The key to calculating the equilibrium is the calculation of the  $P_\theta$  surfaces. It is shown<sup>5,6</sup> that the fluid energy  $E = \gamma mc^2 + q\phi$  and  $g \equiv rB_\theta$  are constant on the  $P_\theta$  level curves, and that the  $P_\theta(r, z)$  surfaces can be found by specifying the dependence of  $E$  and  $g$  on  $P_\theta$ . For parameters that vary slowly compared with the poloidal drift period, the evolution of the beam may be considered adiabatic. The

adiabatic constants of the motion are  $P_\theta$  itself, and the toroidal flux enclosed by a  $P_\theta$  curve,  $\phi_t(P_\theta)$ . (Because we assume that the beam is cold, the third invariant, the magnetic moment  $\mu$  is zero.) These two constants of the motion determine the evolution of  $E(P_\theta, t)$  and  $g(P_\theta, t)$ , and thus generate an evolving series of  $P_\theta$  surfaces.

In a previous work<sup>5,6</sup> the behavior of the equilibria during flux diffusion and acceleration was presented for a modified betatron with rectangular boundaries. In this paper, we present results for a circular boundary (relevant to the current NRL design) and use a modified version of the original iterative computer code in which the outer loop iterations have been accelerated with a fast direct elliptic solver. We find no radically different results in this new geometry. If the beam is positioned exactly right in the chamber, it can survive flux diffusion. However, in practice the beam cannot be exactly positioned, so flux-compensation coils are required. We test the sensitivity of the equilibrium during flux diffusion to errors in currents in the compensating coils. The beam is much more sensitive to errors in current distribution at high current than at low current. However, this sensitivity to field errors is much smaller than in the previously studied case with rectangular boundaries. In addition, the window of acceptable field indices for acceleration is wider because of the shape of the new confining wall, and a much larger volume of parameter space is examined here than in our previous work.

After injection and trapping, the beam in the modified betatron is accelerated in three phases: (1) preacceleration, (2) diffusion, and (3) main acceleration. We will deal with the diffusion and acceleration phases since they occur on time scales of at least two orders of magnitude greater than the poloidal drift period. In our discussion of diffusion, we will examine the effect of imperfect flux diffusion compensation on beam equilibria. A discussion of the numerical-solution procedure and the new elliptic solver can be found in the appendix.

## II. FLUX DIFFUSION

### (a) Constant Energy

Flux diffusion is simulated in our system by specifying the boundary conditions on the flux,  $\psi = rA_\theta$ , as

$$\psi(r, z) = \psi_e(r, z) + \epsilon\psi_r(r, z) + \psi_0, \quad (1)$$

where  $\psi_r$  is the well-known flux of a thin ring carrying beam current  $I^{11}$ ,  $\psi_e$  is due to the external vertical field coils and the constant  $\psi_0$  is determined so that  $P_\theta$  at the reference orbit is conserved. The constant  $\epsilon$  reflects the degree of diffusion;  $\epsilon = 0$  represents no flux diffused and  $\epsilon = 1$  full flux diffusion. The flux  $\psi_0$  is the additional flux through the major orbit that must be provided by external coils. In this set of calculations, the energy of the beam is held constant while the vertical field is adjusted appropriately to hold the beam at the initial equilibrium radius  $r_0$ , as discussed in Refs. [5] and [6]. In the first of these runs,  $r_0 = 100$  cm, the field index,  $\eta = 0.5$ , and as shown in Fig. 2, we find that the vertical field  $B_v$  increases 20% from  $B_v = 120$  G with no flux diffused, to  $B_v = 155$  G with all the flux diffused;  $\psi_0$  also increases during diffusion from 0 to  $2.36 \times 10^5$  G-cm<sup>2</sup>, but  $\psi(r_0)$  remains almost constant. We shall explain the

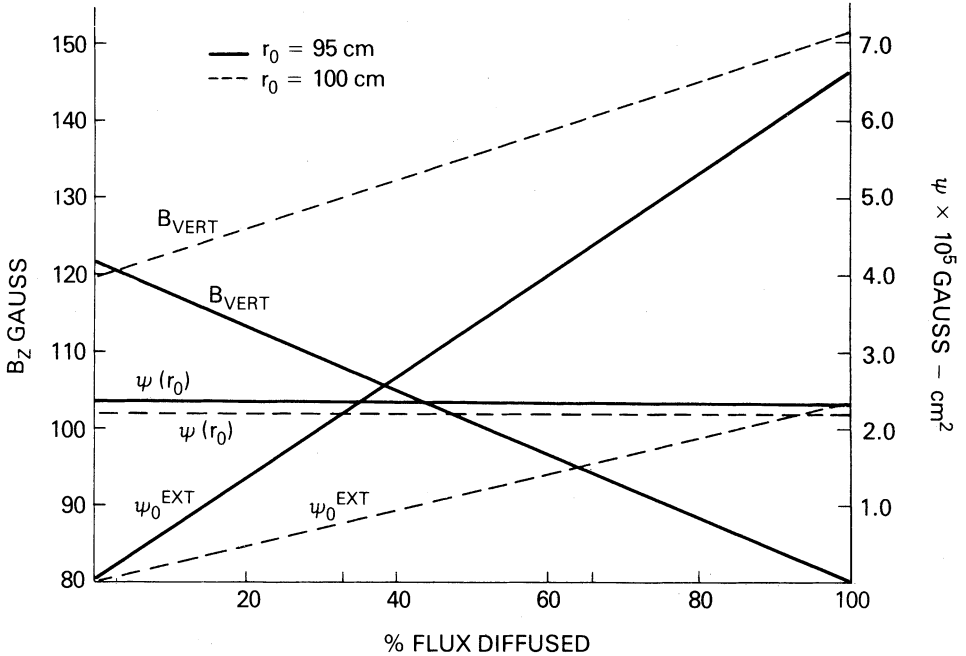


FIGURE 2 Flux diffusion at constant energy.

interdependence of these variables shortly. In Fig. 3 we show the  $P_\theta$  surfaces before and after flux diffusion. The  $x$ -point at approximately 90 cm hardly moves toward the beam at all, so there is no threat of transition to the paramagnetic curves outside the separatrix. This then contrasts to our findings with rectangular geometry where the separatrix moves in during diffusion, ultimately disrupting the equilibrium.

If flux diffusion were to occur with a centered beam and constant external fields, the beam would lose energy and its equilibrium radius would decrease because the decrease in equilibrium radius associated with the reduction of  $\gamma_0$  is greater than the increase in equilibrium radius associated with the enhanced image forces.<sup>7</sup> (The  $1/\gamma^2$  cancellation of image charge forces and image current forces is weaker for smaller  $\gamma$ ). In our calculations, energy and equilibrium radius are fixed, so the vertical field increases to prevent the increase in  $r_0$  produced by the enhanced outward hoop and image forces.

In the next run, we set  $r_0 = 95$  cm and find that  $B_v$  decreases from  $B_v = 121$  G to  $B_v = 81$  G during flux diffusion, while  $\psi_0$  increases from 0 to  $6.62 \times 10^5$  G-cm<sup>2</sup> (see solid lines in Fig. 2). The  $P_\theta$  surface after diffusion is shown in Fig. 4. This time the separatrix does move closer to the beam, from about 4 cm to 1 cm away when flux has diffused, but again the beam is not disrupted.

The explanation for the decrease in  $B_v$  is connected to the shift in the self magnetic field during diffusion. As the repelling image currents in the wall decay, the net forces on the beam point inward due to the electrostatic attraction to the inner (nearer) wall. Thus the imposed inward force, that from  $B_v$ , must also decrease to maintain  $r_0$ . The external flux ( $\psi_0$ ) again increases to compensate for the loss of self flux and  $B_v$  flux at the beam: Thus the question of how  $B_v$  must change during flux diffusion is extremely sensitive to beam position.

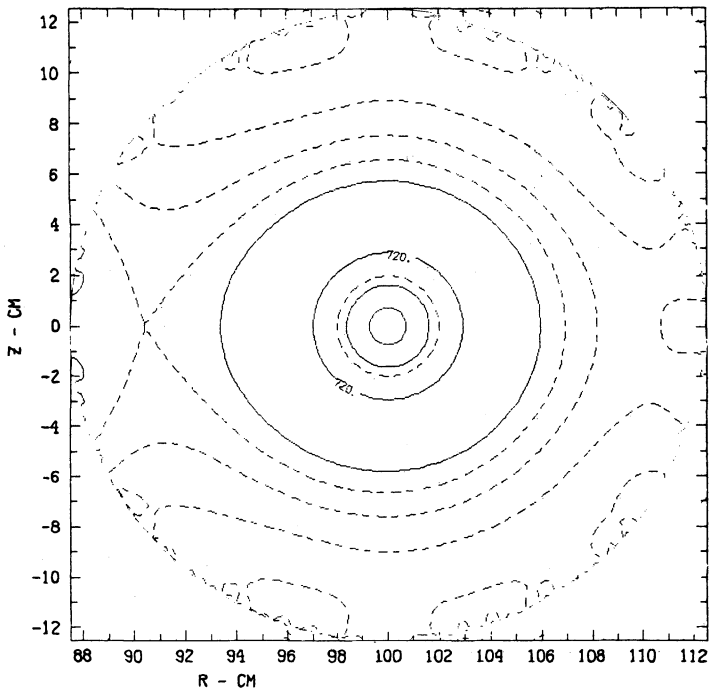
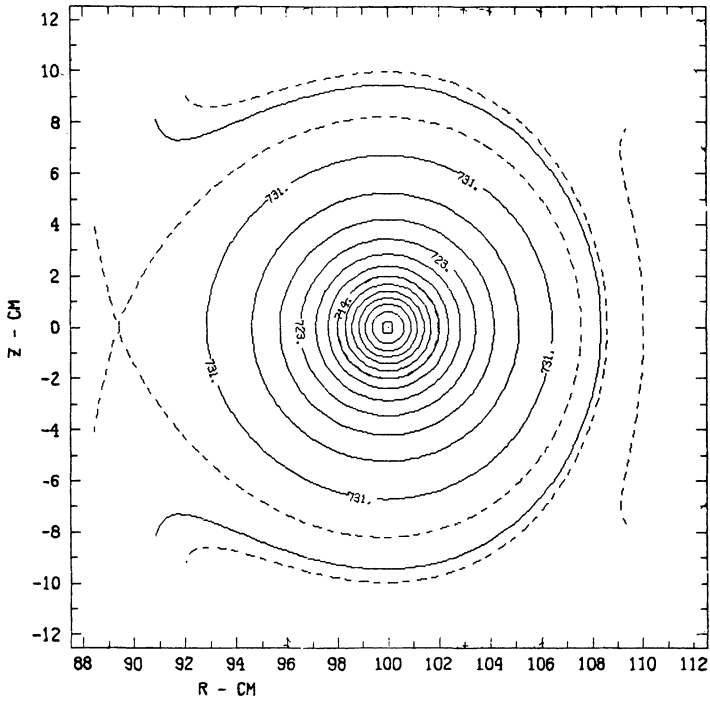


FIGURE 3  $P_0$  topologies during flux diffusion. In 3(a)  $\epsilon = 0$ , in 3(b)  $\epsilon = 1$ .

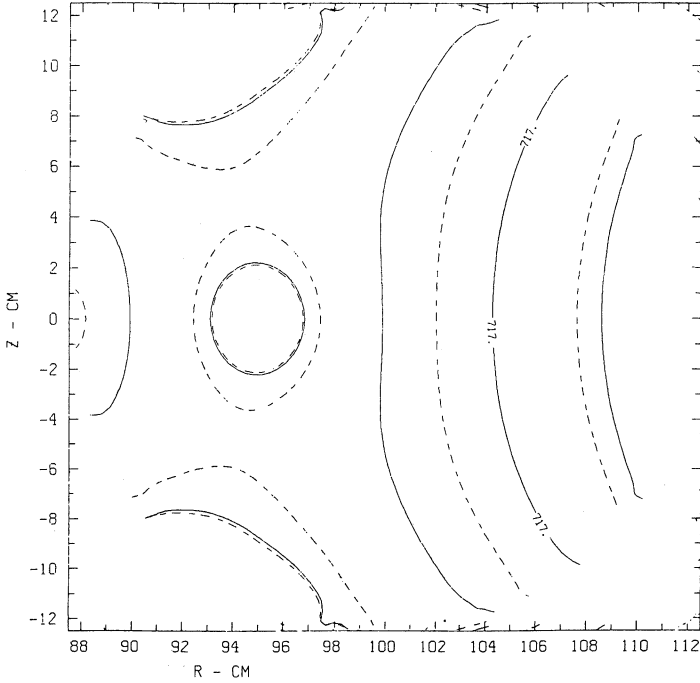


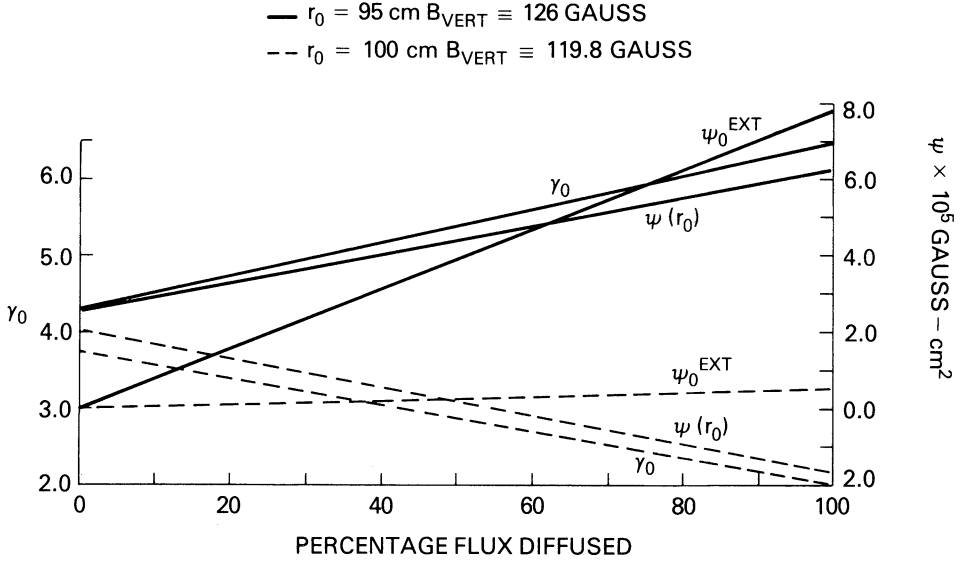
FIGURE 4  $P_\theta$  topology with flux diffusion at  $r_0 = 95$  cm,  $\epsilon = 1$ .

(b) *Constant Vertical Field*

In another set of runs, we diffuse the self flux, but fix  $B_v$  and allow the energy to adjust during diffusion. As in the fixed-energy results, the separatrix does not move closer to the beam when  $r_0 = 100$  cm, but comes within 0.25 cm of the beam when  $r_0 = 95$  cm. Since the separatrix in the latter case hits the wall of the torus, this is a potentially dangerous situation, and beam disruption is likely to occur for beam with  $r_0 = 95$  cm. In Fig. 5, we show the effect on beam energy  $\gamma_0$ , on flux  $\psi(r_0)$ , and on the external flux  $\psi_0$  of flux diffusion with constant vertical field  $B_v$ . At  $r_0 = 100$  cm, the energy decreases during diffusion, from  $\gamma_0 = 3.8$  to  $\gamma = 2.0$ , to counter the increased outward (in the  $\hat{r}$  direction) forces on the beam. At  $r_0 = 95$  cm, the energy increases during diffusion, from  $\gamma = 4.3$  to  $\gamma = 6.45$ . This time the net force from the image currents is outward and its loss must be compensated by increased centrifugal forces.

When the flux diffuses at constant energy,  $\psi(r_0)$  remains nearly constant but  $B_v$  changes dramatically (Fig. 2). With flux diffusion at constant  $B_v$ ,  $\gamma_0$  and  $\psi(r_0)$  both change dramatically (Fig. 5). In fact, during flux diffusion, our results show that  $\gamma_0$  and  $\psi(r_0)$  are related linearly, exactly as they are during acceleration. This follows because  $P_\theta = rm\gamma v_\theta - e\psi$  is a constant of the motion, and  $r$  and  $v_\theta (\approx c)$  are almost constant during flux diffusion. The behavior of  $\psi_0$  (which must be supplied externally) in Figs. 2 and 5 can be directly inferred from the behavior of  $\psi(r_0)$ . The change in flux at beam center is produced by three effects

$$\Delta\psi(r_0) = \Delta\psi_e + \Delta\psi_f + \Delta\psi_0, \quad (2)$$


 FIGURE 5 Flux diffusion with constant  $B_{\text{vert}}$ .

where  $\psi_e$  is the flux due to the vertical field,  $\psi_f$  is due to self-flux (which can change because of diffusion through the walls or because of a change in beam parameters) and  $\psi_0$  is the constant external flux. During flux diffusion at constant energy,  $\psi(r_0)$  is almost constant and  $\psi_0$  maintains  $\psi(r_0)$  by compensating for the loss of self-flux and the loss or gain of flux from the increasing or decreasing  $B_v$  field (Fig. 2). During flux diffusion with constant  $B_v$ ,  $\psi(r_0)$  is tied to  $\gamma_0$  and  $\psi_0$  again must supply the necessary flux according to Eq. (2) (Fig. 5).

### III. FLUX-DIFFUSION COMPENSATION

Because it may not be possible to adjust the vertical field rapidly enough to maintain equilibrium, and furthermore, because the proper increase in  $B_v$  or  $\psi_0$  with  $\epsilon$  is extremely sensitive to the beam position in the linear, it has been proposed that a discrete set of coils be used to compensate for the decay of eddy currents. In this section, we simulate the results of an error in this process of compensation.

We suppose that the set of external conductors is placed along the minor cross section of the torus having a poloidal distribution resembling the distribution of wall currents in a perfect conductor. We suppose further that the error made in this compensation produces a sinusoidal variation of flux at the boundary (the self-flux at the boundary would be identically zero if compensation were perfect). Then the boundary condition on  $\psi$  becomes

$$\psi = \psi_e + \epsilon \tilde{\psi} + \psi_0, \quad (3)$$

where  $\tilde{\psi}$  oscillates along the walls; that is

$$\tilde{\psi}(r, z) = \psi_m \cos 16\phi, \quad (4)$$

where  $\psi_m$  is the maximum value of  $\psi$ , and  $\phi$  signifies the poloidal angle.

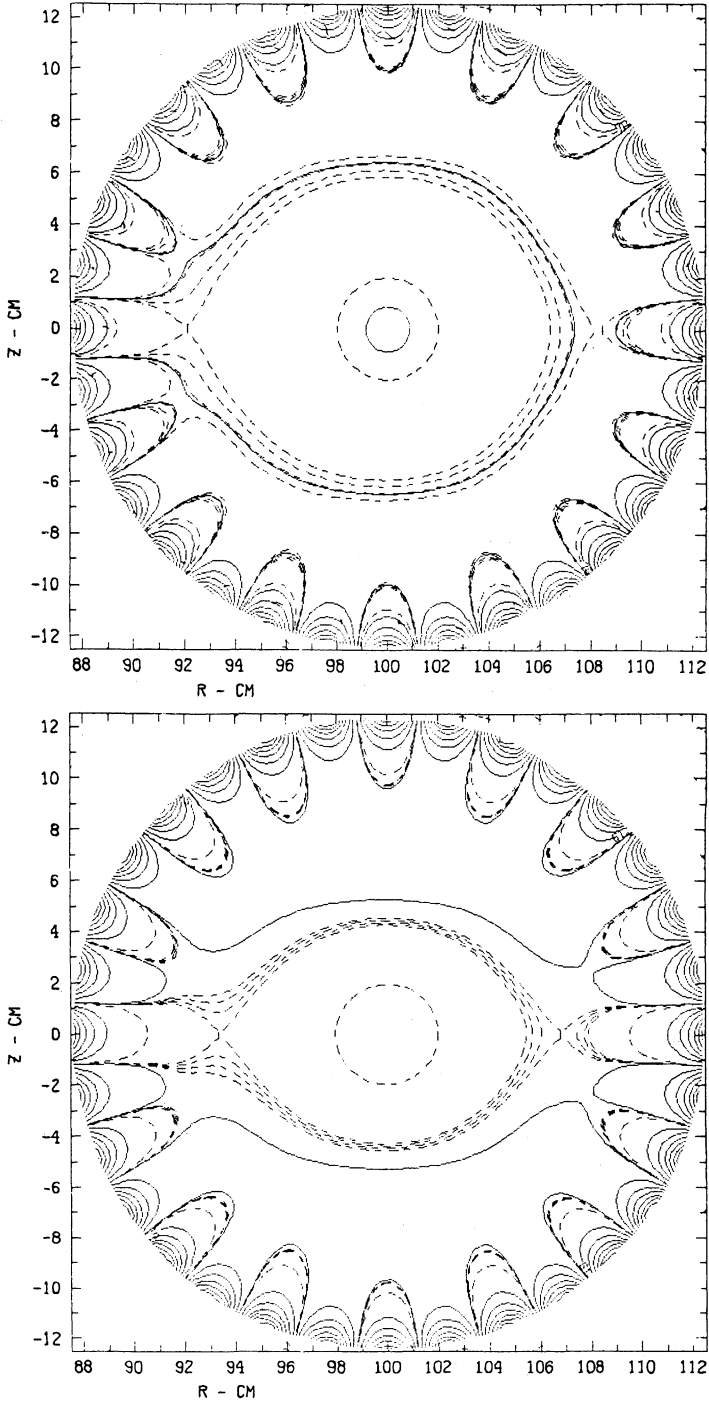


FIGURE 6  $P_\theta$  topologies with flux-compensation coils. In 6(a)  $\epsilon = 0.25$ , in 6(b)  $\epsilon = 1.0$ .



Figure 6 shows the results for  $\epsilon = 0.25$  and  $1.0$ . These curves should be compared to Fig. 3a which corresponds to  $\epsilon = 0$ . The presence of the coils is markedly seen in Fig. 6a, but the distance between the separatrix and the beam decreases only by 1.5 cm between  $\epsilon = 0.25$  and  $\epsilon = 1.0$ , and the separatrix remains well away from the beam. Furthermore, and in contrast to our previous constant-energy flux-diffusion results, the vertical field  $B_v$  increases only 0.83% between  $\epsilon = 0$  and  $\epsilon = 1$ . These results are very optimistic in that they show that the beam is not affected by flux diffusion as long as the diffusion is compensated by the discrete coils. Furthermore, the beam is not sensitive to the level of discretization error.

#### IV. POLOIDAL ERROR

Next we consider the possibility that an error is made in the poloidal distribution of currents in the coils described above. Suppose this error is represented with the following boundary condition on  $\psi$

$$\psi(r, z) = \psi_e + \tilde{\psi} + \epsilon\psi_m \cos \phi + \psi_0, \quad (5)$$

where again  $\psi_m$  is the maximum value of flux produced by a thin ring of current carrying beam current  $I$ , and  $\phi$  signifies poloidal angle. As shown in Fig. 7, we find that both the vertical field necessary to maintain the equilibrium radius and the external flux  $\psi_0$  are very sensitive to these poloidal errors, and that this sensitivity increases with beam current. Equivalently, one would find that for a fixed external field, the equilibrium radius is very sensitive to the degree of poloidal error. The change in  $B_v$  for 5% poloidal error is 18% for  $I = 10$  kA, 8% for  $I = 3$  kA, and 3% for  $I = 1$  kA. Thus when compensating for flux diffusion with external coils, it is essential that poloidal errors in current distribution in these coils be very small.

#### V. ACCELERATION

To treat acceleration of beam, we assume perfect flux diffusion compensation, and increment  $E_0$ , the energy at the equilibrium radius (or 0-point of the  $P_\theta$  surface). As in the rectangular geometry, we find that because of the increased focusing forces and cancellation of electric and magnetic self forces, the separatrix moves in toward the beam as its energy increases. Ultimately the separatrix hits the outer edge of the beam and the transition from diamagnetic to paramagnetic motion occurs. The beam will almost certainly not survive this transition if the separatrix intersects the linear wall.

We now find that as  $\gamma_0$  increases from about 4 to 10 (the transition energy), the orbit is confined during the transition for  $0.4 \leq \eta \leq 0.6$ , but is not confined for field index  $\eta = 0.3$  or  $\eta = 0.7$ . The  $P_\theta$  topology for two field indices,  $\eta = 0.5$  and  $\eta = 0.7$  is shown in Fig. 8 just before the edge of the beam undergoes transition. In the  $\eta = 0.5$  case, the energy  $\gamma_0 = 9.26$ , and the separatrix is well contained in the linear. In the  $\eta = 0.7$  case, the energy  $\gamma_0 = 8$ , and the separatrix (in this case a hidden level curve with two  $x$  points at  $r = 99$  cm,  $z = \pm 4$  cm) runs into the linear.

At this point a few other considerations are worth mentioning. We have done some acceleration calculations at beam current of 1 kA and found that the beam will survive the paramagnetic transition for a broader range of field indexes (almost as high as  $0.3 \leq \eta \leq 0.7$ ). We have also investigated the consequences of initializing the beam with a much flatter density profile than usual and found no effect.

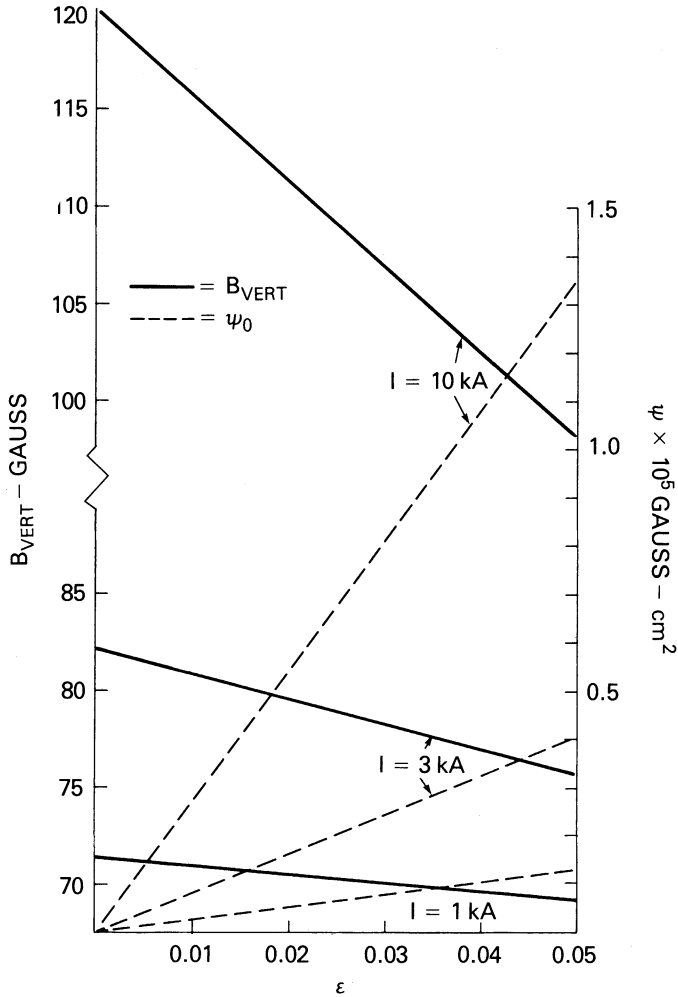


FIGURE 7 Sensitivity of  $B_{\text{vert}}$  and  $\psi_0^{\text{ext}}$  to poloidal errors in flux compensation.

## VI. SUMMARY

The effects of flux diffusion, inadequate flux-diffusion compensation, and acceleration on the beam in the modified betatron have been examined in this paper. Our formalism assumes that the poloidal drift in the toroidal field is well below the Brillouin limit ("slow mode"), that the parameters affecting the beam change adiabatically, and that the beam is cold. This last constraint will be relaxed in a future publication, where we will investigate the effects of transverse emittance on equilibria and adiabatic evolution. We find that beam equilibrium can be lost during flux diffusion unless the diffusion is accurately compensated. Specifically, not only must the total current in the coils cancel the beam current, but even the current distribution in the wall must be accurately modeled. The sensitivity of the beam to current distribution error goes from relatively insensitive for a 1-kA beam to very sensitive for a 10-kA beam. We also find

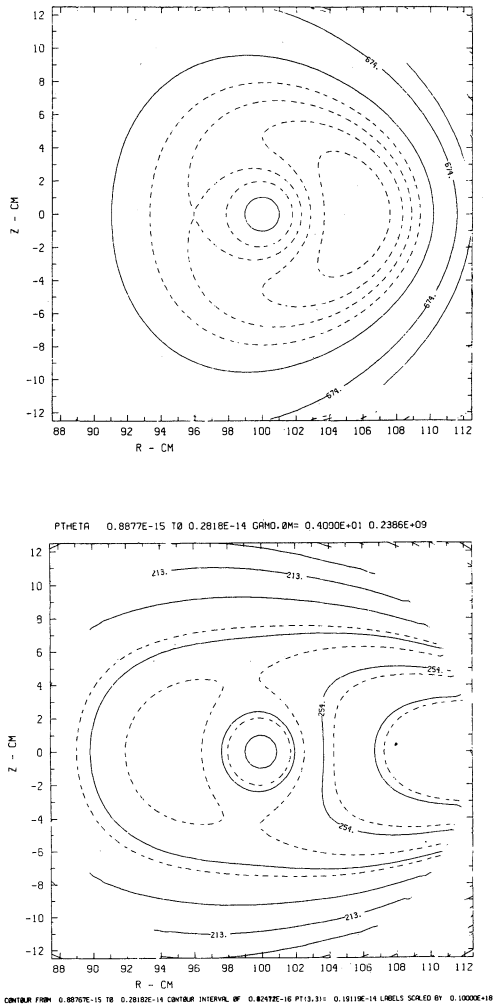


FIGURE 8 Effect of the field index  $\eta$  on  $P_0$  topologies. In 8(a)  $\eta = 0.5$ , in 8(b)  $\eta = 0.7$ .

that a 10-kA beam will survive the diamagnetic to paramagnetic transition provided the field index is within the limits  $0.4 \leq \eta \leq 0.6$ .

ACKNOWLEDGMENTS

We have benefitted from discussions with C. A. Kapetanacos and S. J. Marsh.

REFERENCES

1. N. Rostoker, *Particle Accelerators*, **5**, 93 (1973).
2. P. Sprangle and C. A. Kapetanacos, *J. Appl. Phys.*, **49**, 1 (1978).
3. N. Rostoker, *Comm. Plasma Phys.*, **6**, 91 (1980).

4. D. P. Chernin and P. Sprangle, *Particle Accelerators*, **12**, 85 (1982).
5. W. M. Manheimer and J. M. Finn, *Particle Accelerators*, **14**, 29 (1983).
6. J. M. Finn and W. M. Manheimer, *Phys. Fluids*, **26**, 3400 (1983).
7. C. A. Kapetanacos, P. Sprangle, D. P. Chernin, S. J. Marsh, and I. Haber, *Phys. Fluids*, **26**, 6 (1983).
8. C. A. Kapetanacos, P. Sprangle, and S. J. Marsh, *Phys. Rev. Lett.*, **49**, 741 (1982).
9. P. Sprangle, C. A. Kapetanacos, and S. J. Marsh, *Proc. of Int. Conf. on High Power Electron and Ion Beam Research and Technology*, Palaiseau, France, June 29–July 3, 1981, p. 803.
10. T. P. Hughes, M. M. Campbell, and B. B. Godfrey, *Bull. Am. Phys. Soc.*, **28**, 1040 (1983).
11. J. D. Jackson, *Classical Electrodynamics* (John Wiley and Sons, 2nd Ed, 1962), 177.
12. H. Grad and H. Rubin, *Proc. of the 2nd Int. Conf. on Peaceful Uses of Atomic Energy* (United Nations, Geneva, 1958), Vol. 31, p. 190.
13. H. Grad, *Phys. Fluids*, **10**, 137 (1967).
14. H. Grad, P. N. Hu, and D. C. Stevens, *Proc. Nat. Acad. Sci. USA*, **72**, 3789 (1975).
15. R. W. Hockney, *Methods in Computational Physics*, **9**, 135 (1970).
16. O. Buneman, Rep. SUIPR-294, Institute for Plasma Research, Stanford Univ., Stanford, CA (1969).
17. J. A. George, Rep. STAN-CS-70-159, Computer Science Dept., Stanford Univ., Stanford, CA (1970).
18. B. L. Buzbee, F. W. Dorr, J. A. George, and G. H. Golub, *SIAM J. Numer. Anal.*, **8**, 722 (1971).

## APPENDIX

### Description of the Iterative Equilibrium Code

In this appendix, we discuss the equations governing the self-consistent equilibrium of a modified betatron, and give an outline of the solution procedure. Our method is reminiscent of that used by Grad for calculating the adiabatic compression of a two-dimensional plasma.<sup>12-14</sup>

The cold-fluid equation of motion for the beam in equilibrium is

$$v \cdot \nabla p = q \left( v \times \frac{B}{c} - \nabla \phi \right) \quad (6)$$

where  $p = \gamma m v$   $\gamma$  is the relativistic factor  $(1 - v^2/c^2)^{1/2}$ ,  $B$  is the magnetic induction, and  $\phi$  the scalar potential. By toroidal symmetry, we can write

$$B = \nabla \psi \times \nabla \theta + g \nabla \theta, \quad (7)$$

where  $\psi = r A_\theta$  is the poloidal flux,  $A_\theta$  the toroidal component of the vector potential,  $g = r B_\theta$ , and  $\theta$  the toroidal angle. Using Ampere's law and the toroidal component of Eq. (6), we can show that the level curves of the toroidal canonical angular momentum

$$P_\theta = \gamma m r v_\theta + q \psi / c \quad (8)$$

constitute drift surfaces of the electrons in the poloidal plane and that

$$g = g(P_\theta). \quad (9)$$

If poloidal inertia and centrifugal force are ignored, the poloidal component of Eq. (6) implies that the energy

$$E = \gamma m c^2 + q \phi \quad (10)$$

is a function of  $P_\theta$ , and that

$$\frac{v_\theta}{r} - \frac{g}{4\pi nr^2} \frac{dg}{dP_\theta} = \frac{dE}{dP_\theta} \equiv \Omega(P_\theta), \quad (11)$$

where  $n(r, z)$  is the density.

Defining  $K(P_\theta) = g(dg/dP_\theta)$ , we can rewrite Eq. (11) for the density,

$$n = \frac{K(P_\theta)}{4\pi r^2 [v_\theta/r - \Omega(P_\theta)]}. \quad (12)$$

Finally we compute the electrostatic potential  $\phi$  and poloidal flux  $\psi$  from

$$\nabla^2 \phi = 4\pi ne \quad (13)$$

$$\nabla^* \psi = 4\pi n e r v_\theta / c, \quad (14)$$

where  $\nabla^* \psi = r^{-2} \nabla \cdot (r^{-2} \nabla \psi)$ , and the boundary conditions for acceleration are those of a conducting wall;  $\phi = 0$  and  $\psi = \psi_e + \psi_0$  where  $\psi_e$  is the flux due to the external vertical-field coils and  $\psi_0$  is a constant. For flux diffusion, we model the flux on the boundary to be

$$\psi = \psi_e(r, z) + \epsilon \psi_r(r, z) + \psi_0, \quad (15)$$

where  $\psi_r$  is the well-known flux due to a thin ring carrying beam current  $I$ , and  $\epsilon$  is a measure of how much flux has diffused. For both acceleration and flux diffusion,  $\psi_0$  is an externally imposed constant flux chosen so that  $P_\theta$  at the reference orbit is conserved.  $\psi_0$  must be supplied by an external coil to maintain equilibrium during flux diffusion or acceleration, and is defined to be zero at the first equilibrium.

The elliptic Eqs. (13) and (14) are solved using a special fast Fourier technique that is able to handle circular (or more general) boundaries. The general idea is to solve the elliptic equations in a rectangular region enclosing the actual boundary. In this rectangular region, the usual technique of Fourier transforming in one direction and solving the resulting tridiagonal system in the other direction works. Next a ‘‘Green’s function’’ matrix is generated that computes the discrete surface charges on the real boundary necessary to produce the desired potential (or flux) there.<sup>15–17</sup> This approach can also be interpreted as a method of permuting the matrix obtained by standard finite difference in the disc to a matrix on which the standard FFT methods will work.<sup>18</sup> In this elegant framework, Neumann boundary conditions on irregular regions can also be dealt with easily.

In our computer code, Eqs. (8)–(14) are solved iteratively for the given experimental parameters such as beam current, radius, energy, etc., and for given values of boundary conditions on  $\phi$  and  $\psi$ . Beam equilibrium at any point later in the acceleration or flux diffusion cycle can be found merely by specifying the energy of the beam or the boundary conditions on  $\psi$ . The new equilibrium is found by conserving the adiabatic constants of the motion.